

Two Quantum Cluster Approximations

Th. A. Maier¹, O. Gonzalez^{1,2}, M. Jarrell¹, and Th. Schulthess²

¹ University of Cincinnati
Cincinnati OH 45221, USA

² Computational Material Sciences Group
Oak Ridge National Laboratory
Oak Ridge, TN 37831, USA

Abstract. We provide microscopic diagrammatic derivations of the Molecular Coherent Potential Approximation (MCA) and Dynamical Cluster Approximation (DCA) and show that both are Φ -derivable. The MCA (DCA) maps the lattice onto a self-consistently embedded cluster with open (periodic) boundary conditions, and therefore violates (preserves) the translational symmetry of the original lattice. As a consequence of the boundary conditions, the MCA (DCA) converges slowly (quickly) with corrections $\mathcal{O}(1/L_c)$ ($\mathcal{O}(1/L_c^2)$), where L_c is the linear size of the cluster. However, local quantities, when measured in the center of the MCA cluster, converge more quickly than the DCA result. These results are demonstrated numerically for the one-dimensional symmetric Falicov-Kimball model.

Introduction

One of the most active areas in condensed matter physics is the search for new methods to treat chemically disordered and correlated systems. In these systems, especially in three dimensions or higher, approximations which neglect long ranged correlations are generally thought to provide a reasonable first approximation for many properties.

Perhaps the most successful of these methods are the Coherent Potential Approximation (CPA) [1] and the Dynamical Mean Field Approximation (DMFA) [2,3,4,5], for disordered and correlated systems, respectively. Although these approximations have different origins, they are formally related. Both are single site theories where non-local effects of disorder and correlations are treated in a mean field approximation. Diagrammatically, both the DMFA [3] and the CPA [6] may be defined as theories which completely neglect momentum conservation at all internal vertices. When this principle is applied, the diagrammatic expansion for the irreducible quantities in each approximation collapses onto that of a self-consistently embedded impurity problem.

Many researchers have actively searched for a technique to restore non-local corrections to these approaches. Here, we discuss just two approaches which are fully causal and self-consistent: the Molecular Coherent Potential Approximation (MCA) [7,8] and the Dynamical Cluster Approximation (DCA) [9,10,11,6]. Recently the Cellular Dynamical Mean Field Approach

[12] was proposed for ordered correlated systems, while the Molecular Coherent Potential Approximation has traditionally been applied to disordered systems. Since both methods share a common microscopic definition we use the term MCA to refer to both techniques in the following.

While the MCA is traditionally defined in the real space of the lattice, the DCA is traditionally defined in its reciprocal space. In the MCA, the system lattice is split into a series of identical molecules. Interactions between the molecules are treated in a mean-field approximation, while interactions within the molecule are explicitly accounted for. In the DCA, the reciprocal space of the lattice is split into cells, and momentum conservation is neglected for momentum transfers within each cell while it is (partially) conserved for transfers between the cells. These approximations share many features in common: they both map the lattice problem onto that of a self-consistently embedded cluster problem. Both recover the single site approximation (CPA or DMFA) when the cluster size reduces to one and become exact as the cluster size diverges. Both are fully causal [7,10], and provided that the clusters are chosen correctly [6], they maintain the point group symmetry of the original lattice problem. Here, we provide a microscopic diagrammatic derivation of both the MCA and the DCA, and explore their convergence with increasing cluster size.

Formalism

We will employ a diagrammatic formalism to derive the MCA and DCA, assuming that a collection of electrons on a lattice, with Green function $G(\mathbf{k})$ interact through an interaction $V(\mathbf{k})$.

From the Lattice to the Cluster

Since our object is to define cluster methods, we divide the original lattice of N sites into N/N_c clusters (molecules), each composed of $N_c = L_c^D$ sites, where D is the dimensionality. L_c need not be an integer, for example in a two-dimensional square lattice, a diamond cluster with $N_c = 8$ will have $L_c = 2\sqrt{2}$. However, care must be taken so that the clusters preserve the point group symmetry of the original lattice. We use the coordinate $\tilde{\mathbf{x}}$ to label the origin of the clusters and \mathbf{X} to label the N_c sites within a cluster, so that the site indices of the original lattice $\mathbf{x} = \mathbf{X} + \tilde{\mathbf{x}}$. The points $\tilde{\mathbf{x}}$ form a lattice with a reciprocal space labeled by $\tilde{\mathbf{k}}$. The reciprocal space corresponding to the sites \mathbf{X} within a cluster shall be labeled \mathbf{K} , with $K_\alpha = n_\alpha \cdot 2\pi/L_c$ and integer n_α . Then $\mathbf{k} = \mathbf{K} + \tilde{\mathbf{k}}$. Note that $e^{i\mathbf{K}\cdot\tilde{\mathbf{x}}} = 1$ since a component of $\tilde{\mathbf{x}}$ must take the form $m_\alpha L_c$ with integer m_α .

The formal mapping between the full lattice problem and the cluster is accomplished by relaxing the condition of momentum conservation at the

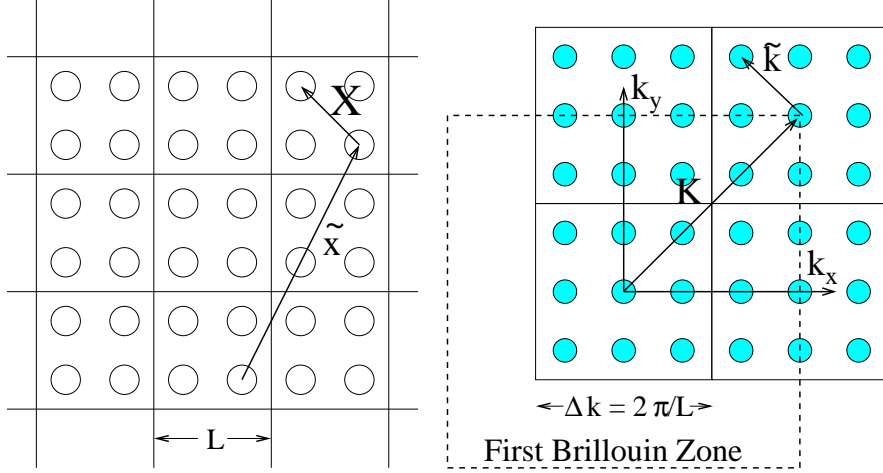


Fig. 1. Definitions of the parameters in real (left) and reciprocal (right) space.

internal vertices of the compact diagrams. Momentum conservation at each vertex is described by the Laue function

$$\Delta = \sum_{\mathbf{x}} e^{i\mathbf{x} \cdot (\mathbf{k}_1 + \mathbf{k}_2 + \dots - \mathbf{k}'_1 - \mathbf{k}'_2 - \dots)} = N \delta_{\mathbf{k}_1 + \mathbf{k}_2 + \dots, \mathbf{k}'_1 + \mathbf{k}'_2 + \dots}, \quad (1)$$

where $\mathbf{k}_1, \mathbf{k}_2$ ($\mathbf{k}'_1, \mathbf{k}'_2$) are the momenta entering (leaving) the vertex. Müller-Hartmann [3] showed that the Dynamical Mean Field (DMF) theory may be derived by completely ignoring momentum conservation at each internal vertex by setting $\Delta = 1$. Then, one may freely sum over all of the internal momentum labels, and the graphs for the generating functional Φ and its irreducible derivatives, contain only local propagators and interactions.

The DCA and MCA techniques may also be defined by their respective Laue functions. In the MCA, we approximate the Laue function by

$$\Delta_{MC} = \sum_{\mathbf{x}} e^{i\mathbf{x} \cdot (\mathbf{K}_1 + \tilde{\mathbf{k}}_1 + \mathbf{K}_2 + \tilde{\mathbf{k}}_2 + \dots - \mathbf{K}'_1 - \tilde{\mathbf{k}}'_1 - \mathbf{K}'_2 - \tilde{\mathbf{k}}'_2 - \dots)}. \quad (2)$$

Thus, the MCA omits the phase factors $e^{i\tilde{\mathbf{k}} \cdot \mathbf{x}}$ resulting from the position of the cluster in the original lattice but retains the (far less important) phase factors $e^{i\tilde{\mathbf{k}} \cdot \mathbf{x}}$ associated with the position within a cluster. In the DCA we also omit the phase factors $e^{i\tilde{\mathbf{k}} \cdot \mathbf{x}}$, so that

$$\Delta_{DC} = N_c \delta_{\mathbf{K}_1 + \mathbf{K}_2 + \dots, \mathbf{K}'_1 + \mathbf{K}'_2 + \dots}. \quad (3)$$

Both the MCA and DCA Laue functions recover the exact result when $N_c \rightarrow \infty$ and the DMFA result, $\Delta = 1$, when $N_c = 1$.

If we apply the MCA Laue function Eq. 2 to diagrams in Φ , assuming that V is a two-particle interaction then each Green function leg is replaced

by the MCA coarse-grained Green function (we have dropped the frequency dependence for notational convenience)

$$\begin{aligned} \bar{G}(\mathbf{X}_1, \mathbf{X}_2; \tilde{\mathbf{x}} = 0) &= \\ \frac{1}{N^2} \sum_{\substack{\mathbf{K}_1, \mathbf{K}_2 \\ \tilde{\mathbf{k}}_1, \tilde{\mathbf{k}}_2}} e^{i(\mathbf{K}_1 + \tilde{\mathbf{k}}_1) \cdot \mathbf{X}_1} G(\mathbf{K}_1, \mathbf{K}_2; \tilde{\mathbf{k}}_1, \tilde{\mathbf{k}}_2) e^{-i(\mathbf{K}_2 + \tilde{\mathbf{k}}_2) \cdot \mathbf{X}_2} &= \\ \frac{N_c^2}{N^2} \sum_{\tilde{\mathbf{k}}_1, \tilde{\mathbf{k}}_2} G(\mathbf{X}_1, \mathbf{X}_2, \tilde{\mathbf{k}}_1, \tilde{\mathbf{k}}_2), \end{aligned} \quad (4)$$

or in matrix notation for the cluster sites \mathbf{X}_1 and \mathbf{X}_2

$$\hat{G} = \frac{N_c}{N} \sum_{\tilde{\mathbf{k}}} \hat{G}(\tilde{\mathbf{k}}), \quad (5)$$

since \hat{G} can be chosen diagonal in $\tilde{\mathbf{k}}_1, \tilde{\mathbf{k}}_2$. Similarly each interaction line is replaced by

$$\begin{aligned} \bar{V}(\mathbf{X}_1, \mathbf{X}_2; \tilde{\mathbf{x}} = 0) &= \\ \frac{1}{N^2} \sum_{\substack{\mathbf{K}_1, \mathbf{K}_2 \\ \tilde{\mathbf{k}}_1, \tilde{\mathbf{k}}_2}} e^{i(\mathbf{K}_1 + \tilde{\mathbf{k}}_1) \cdot \mathbf{X}_1} V(\mathbf{K}_1, \mathbf{K}_2; \tilde{\mathbf{k}}_1, \tilde{\mathbf{k}}_2) e^{-i(\mathbf{K}_2 + \tilde{\mathbf{k}}_2) \cdot \mathbf{X}_2} &= \\ \frac{N_c^2}{N^2} \sum_{\tilde{\mathbf{k}}_1, \tilde{\mathbf{k}}_2} V(\mathbf{X}_1, \mathbf{X}_2, \tilde{\mathbf{k}}_1, \tilde{\mathbf{k}}_2), \end{aligned} \quad (6)$$

or in matrix notation for the cluster sites \mathbf{X}_1 and \mathbf{X}_2

$$\hat{V} = \frac{N_c}{N} \sum_{\tilde{\mathbf{k}}} \hat{V}(\tilde{\mathbf{k}}). \quad (7)$$

The summations of the cluster sites \mathbf{X} within each diagram remain to be performed. \hat{G} and \hat{V} are propagators which are truncated outside the cluster. I.e., if the interaction V is non-local, \hat{V} will include only interactions within, but not between, clusters. Thus the inclusion of the phase factors $e^{i\tilde{\mathbf{k}} \cdot \mathbf{X}}$ in the MCA Laue-function Eq. 2 leads directly to a cluster approach formulated in real space that violates translational invariance. Therefore the Green function and interaction are functions of two cluster momenta $\mathbf{K}_1, \mathbf{K}_2$ or two sites $\mathbf{X}_1, \mathbf{X}_2$ respectively.

If we apply the DCA Laue function Eq. 3, Green function legs in Φ are replaced by the DCA coarse grained Green function

$$\bar{G}(\mathbf{K}) = \frac{N_c}{N} \sum_{\tilde{\mathbf{k}}} G(\mathbf{K}, \tilde{\mathbf{k}}), \quad (8)$$

since Green functions can be freely summed over the $\tilde{\mathbf{k}}$ vectors within a cell about the cluster momentum \mathbf{K} . Similarly, the interactions are replaced by the DCA coarse grained interaction

$$\bar{V}(\mathbf{K}) = \frac{N_c}{N} \sum_{\tilde{\mathbf{k}}} V(\mathbf{K}, \tilde{\mathbf{k}}). \quad (9)$$

As with the MCA, the effect of coarse-graining the interaction is to reduce the effect of non-local interactions to within the cluster. The resulting compact graphs are functionals of the coarse grained Green function $\bar{G}(\mathbf{K})$ and interaction $\bar{V}(\mathbf{K})$, and thus depend on the cluster momenta \mathbf{K} only. For example, when $N_c = 1$, only the local part of the interaction survives the coarse graining. As with the MCA, within the DCA it is important that *both* the interaction and the Green function are coarse-grained [10]. In calculations where a non-local interaction is not coarse-grained, poor results are obtained [13].

From the Cluster to the Lattice

To establish a connection between the cluster and the lattice we minimize the lattice free energy

$$F = -k_B T (\Phi - \text{tr} [\Sigma \mathbf{G}] + \text{tr} \ln [\mathbf{G}]) \quad (10)$$

where Φ is the generating functional composed of all closed compact (single-particle irreducible) graphs, Σ is the lattice self-energy and \mathbf{G} is the full lattice Green function. The trace indicates summation over frequency, momentum and spin. As discussed in many-body texts [14], the additional free energy due to an interaction may be described by a sum over all closed connected graphs. These graphs may be further separated into compact and non-compact graphs. The compact graphs, which comprise the generating functional Φ , consist of the sum over all skeletal graphs (those with no internal parts representing corrections to the single-particle Green function). The remaining graphs comprise the non-compact part of the free energy. In the infinite-dimensional limit, Φ consists of only local graphs, with non-local corrections of order $1/D$. However, for the non-compact parts of the free energy, non-local corrections over arbitrary lengths are of order one, so the local approximation applies only to Φ .

To see this, consider the simplest non-local corrections to non-compact and compact parts of the free energy of a Hubbard-like model, illustrated in Fig. 2. Here the upper (lower) circle is a set of graphs composed of intrasite propagators restricted to site n (the origin). Consider all such non-local corrections on the shell of sites which are n mutually orthogonal unit translations from the origin. In the limit of high dimensions, there are $2^n D! / ((D-n)! n!) \sim \mathcal{O}(D^n)$ such sites. Since as $D \rightarrow \infty$, $G(r) \sim D^{-r/2}$ [2], the legs on the compact correction contribute a factor $\mathcal{O}(D^{-2n})$ whereas those on the non-compact

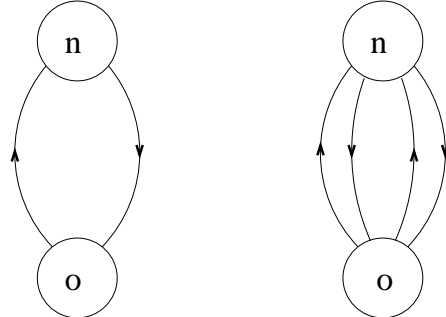


Fig. 2. Non-compact (left) and compact (right) non-local corrections to the free energy functional. Here the upper (lower) circle is meant to represent a set of graphs which are closed except for the external lines shown, and restricted to site n (the origin).

correction contribute $\mathcal{O}(D^{-n})$. Therefore the compact non-local correction falls as D^{-n} and is very short-ranged; whereas, the non-compact correction remains of order one, regardless of how far site n is from the origin [15]. As we will see below, the essential approximation of the DCA and the MCA is to use the cluster propagators, which are accurate only for short distances, to construct various diagrammatic insertions. In high dimensions, or in finite dimensions when the Green functions fall exponentially with distance, this is a good approximation for the compact graphs which comprise Φ , but a poor approximation for the non-compact graphs [15].

Thus, we will approximate the generating functional Φ with its cluster counterpart Φ_c by replacing the Laue function with either Δ_{DC} or Δ_{MC} , but this approximation will not be used in the parts of the free energy coming from non-compact graphs. The free energy then reads

$$F = -k_B T (\Phi_c - \text{tr} [\Sigma \mathbf{G}] + \text{tr} \ln [\mathbf{G}]) \quad (11)$$

F is stationary with respect to \mathbf{G} when $\frac{\delta F}{\delta \mathbf{G}} = 0$. This happens for the MCA if we estimate the lattice self energy as

$$\begin{aligned} \Sigma(\mathbf{K}_1, \mathbf{K}_2; \tilde{\mathbf{k}}_1, \tilde{\mathbf{k}}_2) = & \\ \sum_{\mathbf{X}_1, \mathbf{X}_2} e^{-i(\mathbf{K}_1 + \tilde{\mathbf{k}}_1) \cdot \mathbf{X}_1} \Sigma_{MC}(\mathbf{X}_1, \mathbf{X}_2) e^{i(\mathbf{K}_2 + \tilde{\mathbf{k}}_2) \cdot \mathbf{X}_2}. & \end{aligned} \quad (12)$$

Thus, the corresponding lattice single-particle propagator reads in matrix notation

$$\hat{G}(\tilde{\mathbf{k}}, z) = [zI - \hat{\epsilon}(\tilde{\mathbf{k}}) - \hat{\Sigma}_{MC}(z)]^{-1}, \quad (13)$$

where the dispersion $\hat{\epsilon}(\tilde{\mathbf{k}})$ and self-energy $\hat{\Sigma}_{MC}(z)$ are matrices in cluster real space with

$$[\hat{\epsilon}(\tilde{\mathbf{k}})]_{\mathbf{X}_1 \mathbf{X}_2} = \epsilon(\mathbf{X}_1 - \mathbf{X}_2, \tilde{\mathbf{k}}) \quad (14)$$

$$= \frac{1}{N_c} \sum_{\mathbf{K}} e^{-\mathbf{K} \cdot (\mathbf{X}_1 - \mathbf{X}_2)} \epsilon_{\mathbf{K} + \tilde{\mathbf{k}}}$$

being the intracenter Fourier transform of the dispersion. For the DCA, $\Sigma(\mathbf{k}) = \Sigma_{DC}(\mathbf{K})$ is the proper approximation for the lattice self energy corresponding to Φ_{DC} . The corresponding lattice single-particle propagator is then given by

$$G(\mathbf{K}, \tilde{\mathbf{k}}; z) = \frac{1}{z - \epsilon_{\mathbf{K} + \tilde{\mathbf{k}}} - \Sigma_{DC}(\mathbf{K}, z)}. \quad (15)$$

Both the MCA and DCA are optimized when we equate the lattice and cluster self energies. A similar relation holds for two-particle quantities. Thus, with few exceptions [16], only the irreducible quantities on the cluster and lattice correspond one-to-one.

The MCA (DCA) algorithm, illustrated in Fig. 3, follows directly: We first make an initial guess for the cluster self-energy matrix Σ . This is used with Eqs. 5 and 13 (8 and 15) to calculate the coarse-grained Green function \hat{G} . The cluster excluded Green function $\hat{G}_0 = [\hat{G}^{-1} + \hat{\Sigma}_{MC}]^{-1}$ ($G_0(\mathbf{K}) = [\bar{G}(\mathbf{K})^{-1} + \Sigma_{DC}(\mathbf{K})]^{-1}$) is defined to avoid overcounting self energy corrections on the cluster. It is used to compute a new estimate for the cluster self-energy which is used to reinitialize the process.

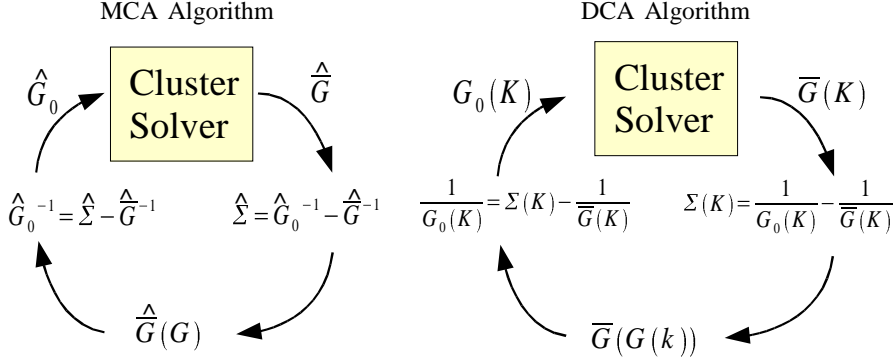


Fig. 3. The MCA and DCA algorithms. The two differ mainly in that in the DCA, the Green functions are diagonal in \mathbf{K} , while in the MCA, they are matrices in the cluster coordinates \mathbf{X} .

Once convergence is reached, the irreducible quantities on the cluster may be used to calculate the corresponding lattice quantities. For example, the cluster self energy and irreducible vertex functions may be used in the Dyson and Bethe-Salpeter equations to calculate the Green function and susceptibilities. In order to obtain a smooth DCA self energy for the calculation of the band structure and spectra, it may be interpolated into the Brillouin

zone of the lattice (however, such interpolation should be avoided during the self-consistency loop, as it may lead to causality violations). The optimal MCA self energy, Eq. 12 is a function of two momenta since the translational invariance of the lattice is violated. Kotliar *et al.*, have introduced a cluster averaging scheme to obtain a self energy as a function of one momenta which may be employed after convergence is obtained [12].

The Small Parameter, $\hat{\Gamma}$: the Coupling Between the Cluster and its Host

In order to compare the character of the two different cluster approaches as a function of the cluster size N_c it is instructive to rewrite the corresponding coarse grained Green-functions Eqs. 5 and 8 to suitable forms by making use of the independence of the self-energy Σ on the integration variable $\tilde{\mathbf{k}}$. For the MCA coarse grained Green function we find

$$\hat{G}(z) = \left[zI - \hat{\epsilon}_o - \hat{\Sigma}_{MC}(z) - \hat{\Gamma}_{MC}(z) \right]^{-1}, \quad (16)$$

with the “cluster-local” energy $\hat{\epsilon}_o = N_c/N \sum_{\tilde{\mathbf{k}}} \hat{\epsilon}(\tilde{\mathbf{k}})$. For the DCA we obtain a similar expression

$$\bar{G}(\mathbf{K}, z) = [z - \bar{\epsilon}_{\mathbf{K}} - \Sigma_{DC}(\mathbf{K}, z) - \Gamma_{DC}(\mathbf{K}, z)]^{-1}, \quad (17)$$

with the coarse grained average $\bar{\epsilon}_{\mathbf{K}} = N_c/N \sum_{\tilde{\mathbf{k}}} \epsilon(\mathbf{K}, \tilde{\mathbf{k}})$. The hybridization functions $\hat{\Gamma}_{MC/DC}(z)$ describe the coupling of the cluster to the mean-field representing the remainder of the system.

The behavior of Γ for large N_c is important. For the MCA, Γ averaged over the cluster sites and frequency

$$\bar{\Gamma}_{MC} = \frac{1}{N_c} \sum_{\mathbf{X}_1, \mathbf{X}_2} \Gamma_{MC}(\mathbf{X}_1, \mathbf{X}_2) \sim \mathcal{O}\left(\frac{2D}{L_c}\right), \quad (18)$$

where $L_c = N_c^{1/D}$ is the linear cluster size. A detailed derivation of this form is presented in the appendix. However, since in the MCA the cluster is defined in real space with open boundary conditions, this form is evident since only the sites on the surface $\propto 2D \cdot L_c^{D-1}$ of the cluster couple to the effective medium and $N_c = L_c^D$. For the DCA we show in the appendix that $\Gamma(\mathbf{K}) \sim \mathcal{O}(1/N_c^{2/D})$ (see also [11]) so that we obtain for the average hybridization of the DCA cluster to the effective medium

$$\bar{\Gamma}_{DC} = \frac{1}{N_c} \sum_{\mathbf{K}} \Gamma_{DC}(\mathbf{K}) \sim \mathcal{O}\left(\frac{1}{L_c^2}\right). \quad (19)$$

The DCA coarse graining results in a cluster in \mathbf{K} -space; thus, the corresponding real space cluster has periodic boundary conditions, and each site in the cluster has the same hybridization strength $\bar{\Gamma}$ with the host.

As shown in the appendix, the average hybridization strength $\bar{\Gamma}$ acts as the small parameter in both the MCA and the DCA. Thus the MCA (DCA) is an approximation with corrections of order $\bar{\Gamma} \sim \mathcal{O}(1/L_c)$ ($\sim \mathcal{O}(1/L_c^2)$).

Numerical Results

To illustrate the differences in convergence with cluster size N_c we performed MCA and DCA simulations for the symmetric one-dimensional (1D) Falicov-Kimball model (FKM). At half filling the FKM Hamiltonian reads

$$H = -t \sum_i (d_i^\dagger d_{i+1} + h.c.) + U \sum_i (n_i^d - 1/2)(n_i^f - 1/2), \quad (20)$$

with the number operators $n_i^d = d_i^\dagger d_i$ and $n_i^f = f_i^\dagger f_i$ and the Coulomb repulsion U between d and f electrons residing on the same site. The FKM can be considered as a simplified Hubbard model with only one spin-species (d) being allowed to hop. However it still shows a complex phase diagram including a Mott gap for large U and half filling, an Ising-like charge ordering with the corresponding transition temperature T_c being zero in 1D, and phase separation in all dimensions. The bare dispersion (in 1D) $\epsilon_k = 2t \cos k$; thus for $t = 1/4$ the bandwidth $W = 1$ which we use as unit of energy. To simulate the effective cluster models of the MCA and the DCA we use a quantum Monte Carlo (QMC) approach described in [10].

To check the scaling relations Eqs. 18 and 19, we show in Fig.4 the average hybridization functions $\bar{\Gamma}_{MC}$ and $\bar{\Gamma}_{DC}$ for the MCA and DCA respectively at the inverse temperature $\beta = 17$ for $U = W = 1$. For $N_c = 1$ both approaches are equivalent to the DMFA and thus $\bar{\Gamma}_{MC} = \bar{\Gamma}_{DC}$. For increasing N_c $\bar{\Gamma}_{MC}$ can be fitted by $0.3361/N_c$ and $\bar{\Gamma}_{DC}$ by $1.1946/N_c^2$ when $N_c > 2$. Cluster quantities, such as the self energy and cluster susceptibilities, are expected to converge with increasing N_c like $\bar{\Gamma}$. This is illustrated in the inset for the staggered ($Q = \pi$) charge susceptibility $\chi_c(\mathbf{Q})$ of the cluster.

Since only the compact parts represented by Φ of the lattice free energy (Eq. 10) are coarse-grained, this scaling is expected to break down when lattice quantities, such as the lattice charge susceptibility, are calculated. The susceptibility of the cluster $\chi_c(Q)$ cannot diverge for any finite N_c ; whereas the lattice $\chi(Q)$ diverges at the transition temperature T_c to the charge ordered phase. Note that the residual mean-field character of both methods can result in finite transition temperatures $T_c > 0$ for finite $N_c < \infty$. However as N_c increases, this residual mean field character decreases gradually and thus increased fluctuations should drive the solution to the exact result $T_c = 0$.

In the DCA [10], $\chi(Q)$ is calculated by first extracting the corresponding vertex function from the cluster simulation. This is then used in a Bethe-Salpeter equation to calculate $\chi(Q)$. T_c is calculated by extrapolating $\chi(Q)^{-1}$ to zero using the function $\chi(Q)^{-1} \propto (T - T_c)^\gamma$ (see inset to Fig.5). This procedure is difficult, if not impossible, in the MCA due to the lack of translational

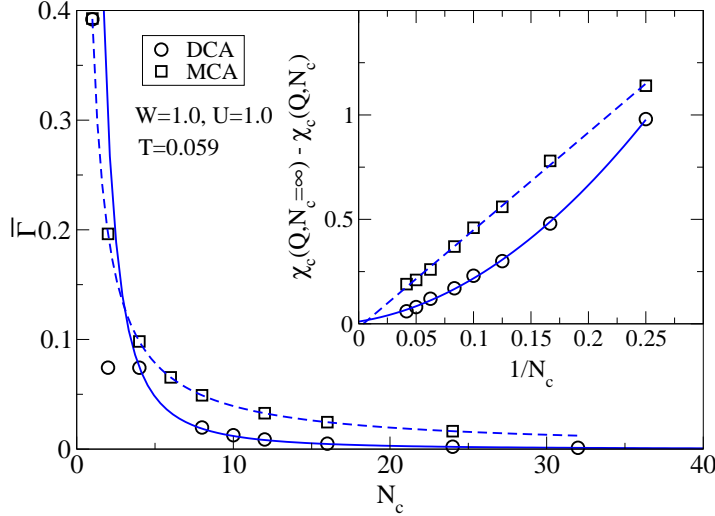


Fig. 4. The average integrated hybridization strengths $\bar{\Gamma}$ of the MCA (squares) and DCA (circles) versus the cluster size N_c when $\beta = 17$ and $U = W = 1$ in the symmetric model. The solid and dashed lines represent the fits $1.1946/N_c^2$ and $0.3361/N_c$ respectively. Inset: Convergence of the cluster charge susceptibility for $Q = \pi$. The solid and dashed lines are quadratic and linear fits, respectively.

invariance. Here, we calculate the order parameter $m(T) = 1/N_c \sum_i (-1)^i \langle n_i^d \rangle$ in the symmetry broken phase. T_c is then obtained from extrapolating $m(T)$ to zero using the function $m(T) \propto (T_c - T)^\beta$. For the DCA this extrapolation is shown by the solid line in the inset to Fig. 5 for $N_c = 4$. The values for T_c obtained from the calculation in the symmetry broken phase and in the unbroken phase must agree, since as we have shown above, both the DCA and MCA are Φ -derivable. This is illustrated in Fig. 5 for the DCA.

A comparison of the DCA and MCA estimate of T_c is presented in Fig. 5. T_c obtained from MCA (squares) is larger than T_c obtained from DCA (circles). Moreover we find that the DCA result seems to scale to zero almost linearly in $1/N_c$ (for large enough N_c), whereas the MCA does not show any scaling form and in fact seems to tend to a finite value for T_c as $N_c \rightarrow \infty$. This striking difference of the two methods can be attributed to the different boundary conditions. The open boundary conditions of the MCA cluster result in a large surface contribution so that $\bar{\Gamma}_{MC} > \bar{\Gamma}_{DC}$. This engenders pronounced mean field behavior that stabilizes the finite temperature transition for the cluster sizes treated here. For larger clusters we expect the bulk contribution to the MCA free energy to dominate so that T_c should fall to zero.

Complementary results are found in simulations of *finite-sized* systems. In general, systems with open boundary conditions are expected to have a surface contribution in the free energy of order $\mathcal{O}(1/L_c)$ [17]. This term is

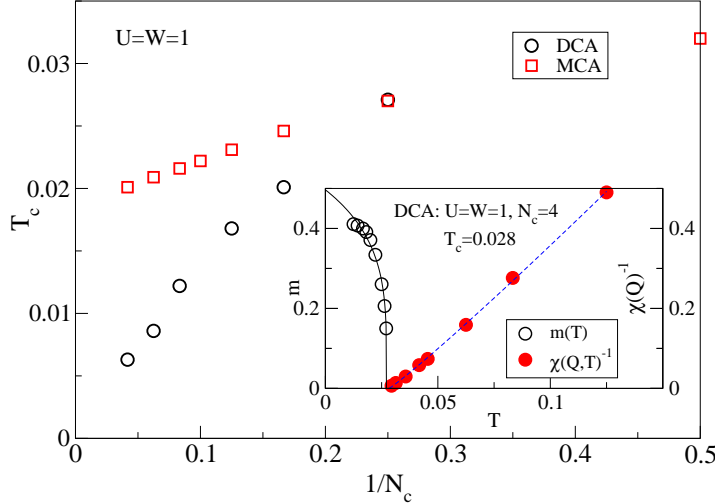


Fig. 5. The transition temperature T_c for the DCA (circles) and MCA (squares) when $U = W = 1$ versus the cluster size N_c . For all values of N_c the DCA prediction is closer to the exact result ($T_c = 0$). Inset: Order parameter $m(T)$ and inverse charge susceptibility $\chi(Q)^{-1}$ versus temperature. The solid (dashed) line represents a fit to the functions $m(T) \propto (T_c - T)^\beta$ with $\beta = 0.245$ ($\chi(T) \propto (T - T_c)^{-\gamma}$ with $\gamma = 1.07$).

absent in systems with periodic boundary conditions. As a result, simulations of finite-sized systems with periodic boundary conditions converge much more quickly than those with open boundary conditions [18].

Thus far, we have shown that the DCA converges more quickly than the MCA for critical properties and for extended cluster quantities (e.g. the cluster susceptibility). This is due to the differences in the boundary conditions, and the coupling to the mean-field. Whereas each site in the DCA experiences the same coupling to the mean-field host, in the MCA only the sites on the boundary of the cluster couple to the host. Provided that the system is far from a transition, the sites in the center of the cluster couple to the mean-field only through propagators which fall exponentially with distance. Thus, one might expect that local results, such as the single-particle density of states, might converge more quickly within the MCA provided that they are measured on these central sites. This is illustrated in Fig. 6 where we plot the single-particle density of states calculated with the DCA and the MCA on the two central sites.

Summary.

By defining appropriate Laue functions, we provide microscopic diagrammatic derivations of the MCA and DCA. We show that they are Φ -derivable,

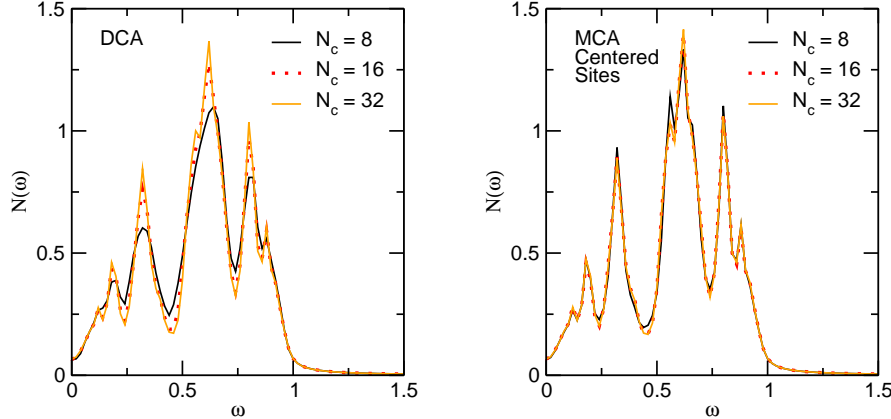


Fig. 6. Comparison of the single-particle density of states (DOS) calculated with the DCA (left) and the MCA (right) on the two central sites for various cluster sizes N_c when $\beta = 10$ and $U = W = 1$ (since the DOS is symmetric around $\omega = 0$, only the $\omega \geq 0$ part is shown). Local quantities, such as the DOS, converge more quickly when calculated on the central sites of the MCA cluster than the cluster averaged DCA result.

and that the lattice free energy is optimized by equating the irreducible quantities on the lattice to those on the cluster. The MCA maps the lattice to a cluster with open boundaries and consequently, the cluster violates translational invariance. In contrast, the DCA cluster has periodic boundary conditions, and therefore preserves the translational invariance of the lattice.

These differences in the boundary conditions translate directly to different asymptotic behaviors for large clusters N_c . As we find analytically as well as numerically, the surface contributions in the MCA lead to an average hybridization $\bar{\Gamma}$ of the cluster to the mean field that scales like $1/L_c$ as compared to the $1/L_c^2$ scaling of the DCA. Since $\bar{\Gamma}$ acts as the small parameter for these approximation schemes, the DCA converges much more quickly than the MCA. These effects are more pronounced near a transition, where the large surface contribution of the MCA stabilizes the mean-field character of the transition. Consequently, the DCA result for the transition temperature T_c of the 1D symmetric FKM model scales almost like $1/N_c$ to the exact result $T_c = 0$, whereas the MCA result converges very slowly. The boundary conditions also differ in that only the MCA sites at the surface of the cluster couple to the mean field; whereas, all DCA cluster sites have an equal coupling to the mean field host. As a result local quantities, such as the density of states, when measured on the central sites of the MCA cluster converge more quickly than than corresponding DCA results.

Thus, for critical properties and extended cluster quantities, the DCA converges far more quickly than the MCA; whereas for local quantities which may be measured at the central sites of the MCA cluster, the MCA converges

more quickly. Since the origin of these differences lies in the different boundary conditions we expect them to hold generally for any model of electrons moving on a lattice.

Acknowledgements We acknowledge useful conversations with N. Blümer, A. Gonis, M. Hettler, H.R. Krishnamurthy, D.P. Landau, Th. Pruschke, W. Shelton, and A. Voigt. This work was supported by NSF grants DMR-0073308 and 0113574. This research was supported in part by NSF cooperative agreement ACI-9619020 through computing resources provided by the National Partnership for Advanced Computational Infrastructure at the Pittsburgh Supercomputer Center.

Appendix

To differentiate the MCA from the DCA we find expressions for the corresponding host-functions Γ . To this end we split the hopping integral t into an inter- and intracluster part. For the MCA the intercluster hopping $[\hat{T}_{MC}]_{\mathbf{x}_1, \mathbf{x}_2} = T_{MC}(\mathbf{X}_1, \mathbf{X}_2)$ is defined as $\hat{T}_{MC}(\tilde{\mathbf{k}}) = \hat{\epsilon}(\tilde{\mathbf{k}}) - \hat{\epsilon}_o$ and reads in real space

$$\hat{T}_{MC}(\tilde{\mathbf{x}}) = \hat{t}(\tilde{\mathbf{x}}) - \hat{\epsilon}_o \delta(\tilde{\mathbf{x}}). \quad (21)$$

Since $\hat{\epsilon}_o = \hat{t}(\tilde{\mathbf{x}} = 0)$, the intercluster hopping matrix $\hat{T}_{MC}(\tilde{\mathbf{x}})$ is only finite for $\tilde{\mathbf{x}} \neq 0$ as expected. Thus, $\hat{T}_{MC}(\tilde{\mathbf{x}})$ has non-vanishing matrix-elements only for sites on the boundary of the cluster. For the DCA the intercluster hopping integral is analogously defined as $T_{DC}(\mathbf{K}, \tilde{\mathbf{k}}) = \epsilon(\mathbf{K}, \tilde{\mathbf{k}}) - \bar{\epsilon}_{\mathbf{K}}$ and can be written in real space as

$$\hat{T}_{DC}(\tilde{\mathbf{x}}) = \hat{t}(\tilde{\mathbf{x}}) - \hat{t} \hat{\delta}^c(\tilde{\mathbf{x}}), \quad (22)$$

where $[\hat{t}]_{\mathbf{x}_1, \mathbf{x}_2} = \bar{t}(\mathbf{X}_1 - \mathbf{X}_2) = 1/N_c \sum_{\mathbf{K}} e^{i\mathbf{K} \cdot (\mathbf{X}_1 - \mathbf{X}_2)} \bar{\epsilon}_{\mathbf{K}}$ and the cluster delta-like function $[\hat{\delta}^c(\tilde{\mathbf{x}})]_{\mathbf{x}_1, \mathbf{x}_2} = \delta^c(\mathbf{X}_1 - \mathbf{X}_2, \tilde{\mathbf{x}}) = N_c/N \sum_{\tilde{\mathbf{k}}} e^{i\tilde{\mathbf{k}} \cdot (\mathbf{X}_1 - \mathbf{X}_2 + \tilde{\mathbf{x}})}$. We have discussed elsewhere that $\delta^c(\mathbf{X}_1 - \mathbf{X}_2, \tilde{\mathbf{x}}) \approx 1$ for $\tilde{\mathbf{x}} = 0$ and falls off rapidly for finite $\tilde{\mathbf{x}}$. It is important to note that $\bar{t}(\mathbf{X}_1 - \mathbf{X}_2) = t(\mathbf{X}_1 - \mathbf{X}_2, \tilde{\mathbf{x}} = 0)$ for $N_c = N$, but $|\bar{t}(\mathbf{X}_1 - \mathbf{X}_2)| < |t(\mathbf{X}_1 - \mathbf{X}_2, \tilde{\mathbf{x}} = 0)|$ for $N_c < N$. It follows that the DCA intercluster hopping $T_{DC}(\mathbf{X}_1 - \mathbf{X}_2, \tilde{\mathbf{x}})$ for $\tilde{\mathbf{x}} = 0$, i.e. between sites belonging to the same cluster, is even finite when $N_c < N$; however it is strongly reduced compared to $\tilde{\mathbf{x}} \neq 0$. This is a consequence of the periodicity of the DCA cluster. Therefore we find that the effective model of the DCA cannot be thought of N/N_c clusters composing the original lattice, but we have to rather think of it as a renormalized model in real space.

Now we proceed with finding expressions for the hybridization functions Γ defined in Eq. (16) and (17) for the MCA and DCA. We start with the MCA. To this end we define a Green function matrix

$$\hat{g}(z) = \left[zI - \hat{\epsilon} - \hat{\Sigma}_{MC}(z) \right]^{-1}, \quad (23)$$

that is localized on the impurity cluster. With this definition Eq. (5) reads

$$\hat{G} = \frac{N_c^2}{N^2} \sum_{\tilde{\mathbf{k}}} \hat{G}(\tilde{\mathbf{k}}) = \left[\hat{g}^{-1} - \hat{\Gamma}_{MC} \right]^{-1}, \quad (24)$$

and Eq. (13) can be rewritten to

$$\hat{G}(\tilde{\mathbf{k}}) = \hat{g} + \hat{g} \hat{\Gamma}_{MC}(\tilde{\mathbf{k}}) \hat{G}(\tilde{\mathbf{k}}). \quad (25)$$

After inserting Eq. (25) into Eq. (24) and using $\sum_{\tilde{\mathbf{k}}} \hat{\Gamma}_{MC}(\tilde{\mathbf{k}}) = 0$ we obtain after some algebraic transformations for the MCA-hybridization matrix

$$\begin{aligned} \hat{\Gamma}_{MC} = & \left[I + \frac{N_c}{N} \sum_{\tilde{\mathbf{k}}} \hat{\Gamma}_{MC}(\tilde{\mathbf{k}}) \hat{G}(\tilde{\mathbf{k}}) \right]^{-1} \times \\ & \frac{N_c}{N} \sum_{\tilde{\mathbf{k}}} \hat{\Gamma}_{MC}(\tilde{\mathbf{k}}) \hat{G}(\tilde{\mathbf{k}}) \hat{\Gamma}_{MC}(\tilde{\mathbf{k}}). \end{aligned} \quad (26)$$

Since, as we pointed out above, \hat{T} has non-zero matrix-elements only between sites on the boundary of the impurity cluster, $\bar{\Gamma}$ is finite only for sites on the boundary but vanishes for sites inside the cluster. Thus, the average hybridization strength of the MCA cluster per site

$$\bar{\Gamma}_{MC} = \frac{1}{N_c} \sum_{\mathbf{X}_1, \mathbf{X}_2} \Gamma_{MC}(\mathbf{X}_1, \mathbf{X}_2) \sim \mathcal{O}\left(\frac{2D}{L_c}\right), \quad (27)$$

since only the sites on the surface $\propto 2D \cdot L_c^{D-1}$ of the cluster couple to the effective medium and $N_c = L_c^D$.

For the DCA we can follow the steps presented above for the MCA since $\Gamma_{DC}(\mathbf{K})$ can be considered a diagonal matrix in \mathbf{K} . We obtain for the DCA hybridization function

$$\Gamma_{DC}(\mathbf{K}) = \frac{\frac{N_c}{N} \sum_{\tilde{\mathbf{k}}} T_{DC}^2(\mathbf{K}, \tilde{\mathbf{k}}) G(\mathbf{K}, \tilde{\mathbf{k}})}{1 + \frac{N_c}{N} \sum_{\tilde{\mathbf{k}}} T_{DC}(\mathbf{K}, \tilde{\mathbf{k}}) G(\mathbf{K}, \tilde{\mathbf{k}})}. \quad (28)$$

It should be stressed that due to the periodicity of the DCA cluster every site of the impurity cluster couples to the effective medium. The momenta $\tilde{\mathbf{k}}$ are restricted to a DCA coarse graining cell and therefore maximal of the order $\mathcal{O}(\Delta k)$, where $\Delta k \propto 1/L$. Since $\epsilon(\mathbf{K}) - \bar{\epsilon}_{\mathbf{K}} \sim \mathcal{O}((\Delta k)^2)$, we find by performing a Taylor series expansion of $T_{DC}(\mathbf{K}, \tilde{\mathbf{k}})$ around $\epsilon(\mathbf{K})$ that $T_{DC}(\mathbf{K}, \tilde{\mathbf{k}}) \sim \mathcal{O}(1/L_c)$. For the overall hybridization of the DCA cluster to the effective medium we thus obtain

$$\bar{\Gamma}_{DC} = \frac{1}{N_c} \sum_{\mathbf{K}} \Gamma_{DC}(\mathbf{K}) \sim \mathcal{O}\left(\frac{1}{L_c^2}\right). \quad (29)$$

In both the DCA and the MCA, the average hybridization strength acts as the small parameter. The approximation performed by the DCA (MCA) is to replace the lattice Green function $G(\mathbf{K}, \mathbf{k}, z) = [z - \epsilon_{\mathbf{K}+\tilde{\mathbf{k}}} - \Sigma(\mathbf{K}, \tilde{\mathbf{k}}, z)]^{-1}$ ($\hat{G}(\tilde{\mathbf{k}}) = [zI - \hat{\epsilon}(\tilde{\mathbf{k}}) - \hat{\Sigma}(\tilde{\mathbf{k}}, z)]^{-1}$) by its coarse grained quantity $\bar{G}(\mathbf{K})$ ($\hat{\bar{G}}$) in diagrams for the generating functional Φ .

According to Eq. (17) the coarse grained Green function of the DCA can be expressed as $\bar{G}(\mathbf{K}, z) = [z - \bar{\epsilon}_{\mathbf{K}} - \Sigma_{DC}(\mathbf{K}, z) - \Gamma_{DC}(\mathbf{K}, z)]^{-1}$. For the time being, assume that $\Sigma_{DC}(\mathbf{K}, z)$ has corrections of the same, or higher, order in $1/L_c$ as the average hybridization strength. Both the self energy and $\epsilon_{\mathbf{K}+\tilde{\mathbf{k}}} = \bar{\epsilon}_{\mathbf{K}} + \mathcal{O}(1/L_c)$ with the leading order corrections being linear in $\tilde{\mathbf{k}}$. Since furthermore $\Gamma_{DC}(\mathbf{K}) \sim \mathcal{O}(1/L_c^2)$, $\bar{G}(\mathbf{K}, \tilde{\mathbf{k}}) \approx \bar{G}(\mathbf{K}) + \mathcal{O}(1/L_c)$. The diagrams for Φ however are summed over $\tilde{\mathbf{k}}$, so that the terms $\sim \mathcal{O}(1/L_c)$ coming from $\epsilon_{\mathbf{K}+\tilde{\mathbf{k}}}$ and similar terms from the self energy vanish and only the terms $\sim \mathcal{O}(1/L_c^2)$, or higher, survive. Thus we find for the DCA that $\Phi \approx \Phi_{DC} + \mathcal{O}(1/L_c^2)$. The corresponding estimate of $\Sigma_{DC}(\mathbf{K}, z)$ will also have corrections $\mathcal{O}(1/L_c^2)$, confirming the assumption above.

According to Eq. (16), the coarse grained propagator of the MCA can be written as $\hat{\bar{G}}(z) = [zI - \hat{\epsilon}_o - \hat{\Sigma}_{MC}(z) - \hat{\Gamma}_{MC}(z)]^{-1}$. If we assume that $\hat{\Sigma}_{MC}$ converges with L_c as fast or faster than $1/L_c$ we see with the L_c -dependence of $\hat{\Gamma}_{MC}$ in Eq. (27) that $\hat{G}(\tilde{\mathbf{k}}) \approx \hat{\bar{G}} + \mathcal{O}(1/L_c)$ since $\hat{\epsilon}(\tilde{\mathbf{k}}) = \hat{\epsilon}_o + \mathcal{O}(1/L_c)$. Thus we obtain for the MCA approximation $\Phi \approx \Phi_{MC} + \mathcal{O}(1/L_c)$ and $\hat{\Sigma}$ will converge with L_c as $\mathcal{O}(1/L_c)$ confirming our assumption.

References

1. D.W. Taylor, Phys. Rev. **156**, 1017 (1967); P. Soven Phys. Rev. **156**, 809 (1967); P.L. Leath and B. Goodman, Phys. Rev. **148**, 968 (1966).
2. W. Metzner and D. Vollhardt, Phys. Rev. Lett. **62**, 324 (1989).
3. E. Müller-Hartmann: Z. Phys. B **74**, 507–512 (1989).
4. T. Pruschke, M. Jarrell and J.K. Freericks, Adv. in Phys. **42**, 187 (1995).
5. A. Georges, G. Kotliar, W. Krauth and M.J. Rozenberg, Rev. Mod. Phys. **68**, 13 (1996).
6. M. Jarrell and H.R. Krishnamurthy, Phys. Rev. B **63**, 125102 (2001).
7. F. Ducastelle, J. Phys. C. Sol. State. Phys. **7**, 1795 (1974).
8. A. Gonis, *Green functions for ordered and disordered systems*, in the series *Studies in Mathematical Physics*, Eds. E. van Groesen and E.M. DeJager, (North Holland, Amsterdam, 1992).
9. M.H. Hettler, A.N. Tahvildar-Zadeh and M. Jarrell, Phys. Rev. B **58**, 7475 (1998).
10. M.H. Hettler, M. Mukherjee, M. Jarrell, and H.R. Krishnamurthy, Phys. Rev. B **61**, 12739 (2000).
11. Th. Maier, M. Jarrell, Th. Pruschke and J. Keller, Eur. Phys. J. B **13**, 613 (2000).
12. G. Kotliar, S.Y. Savrasov, G. Pálsson and G. Biroli, Phys. Rev. Lett. **87**, 186401 (2001). This method reduces to the MCA when non-overlapping clusters are chosen.

13. G. Biroli and G. Kotliar, Phys. Rev. B **65**, 155112 (2002).
14. A.A. Abrikosov, L.P. Gorkov, I.E. Dzyalishinski, *Methods of Quantum Field Theory in Statistical Physics*, (Dover, New York, 1975).
15. K. Aryanpour, M. H. Hettler and M. Jarrell, Phys. Rev. B **65**, 153102 (2002).
16. In both the DCA and MCA, on-site lattice and cluster quantities correspond one-to-one. In the MCA, the single-particle green functions within the cluster and the lattice also correspond.
17. M.E. Fisher and M.N. Barber, Phys. Rev. Lett. **28**, 1516 (1972).
18. D.P. Landau, Phys. Rev. B **13**, 2997 (1976).